Non-equilibrium emission of complex fragments from p+Au collisions at 2.5 GeV proton beam energy

A.Bubak,[1,2] A.Budzanowski,[3] D.Filges,[1] F.Goldenbaum,[1] A.Heczko,[4] H.Hodde,[5] L.Jarczyk,[6] B.Kamys,[6,*] M.Kistryn,[3] St.Kistryn,[4] St.Kliczewski,[3] A.Kowalczyk,[4] E.Kozik,[3] P.Kulessa,[1,3] H.Machner,[1] A.Magiera,[4] W.Migdał,[4] N.Paul,[1] B.Piskor-Ignatowicz,[1,4] M.Puchała,[4] K.Pysz,[1,3] Z.Rudy,[4] R.Siudak,[1,3] M.Wojciechowski,[4] and P. Wüstner[1]

(PISA - **P**roton **I**nduced **S**p**A**llation collaboration)

[1]*Institut für Kernphysik, Forschungszentrum Jülich, D-52425 Jülich, Germany*
[2]*Institute of Physics, Silesian University, Uniwersytecka 4, 40007 Katowice, Poland*
[3]*H. Niewodniczański Institute of Nuclear Physics PAN, Radzikowskiego 152, 31342 Kraków, Poland*
[4]*M. Smoluchowski Institute of Physics, Jagellonian University, Reymonta 4, 30059 Kraków, Poland*
[5]*Institut für Strahlen- und Kernphysik, Bonn University, D-53121 Bonn, Germany*
[6]*M. Smoluchowski Institute of Physics, Jagellonian University, Reymonta 4, 30059 Kraków, Poland*

(Dated: February 1, 2008)

Energy and angular dependence of double differential cross sections $d^2\sigma/d\Omega dE$ was measured for reactions induced by 2.5 GeV protons on Au target with isotopic identification of light products (H, He, Li, Be, and B) and with elemental identification of heavier intermediate mass fragments (C, N, O, F, Ne, Na, Mg, and Al). It was found that two different reaction mechanisms give comparable contributions to the cross sections. The intranuclear cascade of nucleon-nucleon collisions followed by evaporation from an equilibrated residuum describes low energy part of the energy distributions whereas another reaction mechanism is responsible for high energy part of the spectra of composite particles. Phenomenological model description of the differential cross sections by isotropic emission from two moving sources led to a very good description of all measured data. Values of the extracted parameters of the emitting sources are compatible with the hypothesis claiming that the high energy particles emerge from pre-equilibrium processes consisting in a breakup of the target into three groups of nucleons; small, fast and hot fireball of ~ 8 nucleons, and two larger, excited prefragments, which emits the light charged particles and intermediate mass fragments. The smaller of them contains ~ 20 nucleons and moves with velocity larger than the CM velocity of the proton projectile and the target. The heavier prefragment behaves similarly as the heavy residuum of the intranuclear cascade of nucleon-nucleon collisions.

PACS numbers: 25.40-h,25.40.Sc,25.40.Ve
Keywords: Proton induced reactions, spallation, fragmentation

I. INTRODUCTION

The mechanism of proton - nucleus interactions at GeV energies is still not well understood. Even the gold nucleus which is the most frequently studied target, at least as concerns the measurements of *total cross sections* for emission of different products (cf. Refs.[1–9] and references herein), reveals unexpected phenomena when more exclusive observables are investigated. Recently measurements of *differential cross sections* in 4π geometry were undertaken [10, 11] for light charged particles (LCP's), i.e. H and He ions, as well as for intermediate mass fragments (IMF's) - Li and Be ions. The measurements were done at 1.2 GeV proton energy for ^{1,2,3}H, ^{3,4,6}He, ^{6,7,8,9}Li and ^{7,9,10}Be isotopes [10], and at 2.5 GeV for ^{1,2,3}H, ^{3,4}He, and ^{6,7}Li isotopes [11].

It was found that the shape of energy spectra of emitted composite particles as well as their angular dependence cannot be explained using the conventional picture of the intranuclear cascade of nucleon-nucleon collisions followed by fragment evaporation from excited remnant nucleus in competition with fission process. Whereas the low energy part of spectra - up to 60 - 80 MeV - seems to be reasonably well described by this conventional mechanism, the high energy part of spectra is generally strongly underestimated by any of the existing models. It is more flat than the low energy part of the spectrum and its slope increases monotonically with the emission angle. This behavior indicates the necessity to include non-equilibrium processes in the description of the reaction mechanism. Authors of Refs. [10–12] propose the surface coalescence of emitted nucleons as process responsible for high energy part of the ^{2,3}H and ^{3}He spectra. They claim, however, that such a mechanism is ruled out for ^{4}He and heavier ejectiles [10, 11].

In the present study the task was undertaken to measure double differential cross sections ($d^2\sigma/d\Omega dE$) with isotopic identification of the light reaction products from proton - gold collisions at proton beam energy of 2.5 GeV, extending the range of detected ejectiles to heavier than those from previous reported investigations [10, 11].

It should be emphasized that for the gold target the

*Electronic address: ufkamys@cyf-kr.edu.pl [corresponding author]

double differential cross sections ($d^2\sigma/d\Omega dE$) of intermediate mass fragments, i.e. fragments with mass number $A_F > 4$, were not measured up to now with isotopic identification . The only available data are published by Letourneau et al. [11] for ^{6,7}Li. Low statistics of isotopically identified data in publication of Herbach et al. [10] did not allow to analyze double differential cross sections ($d^2\sigma/d\Omega dE$) for isotopes heavier than ^{4}He. For individual isotopes only the analysis of angle integrated ($d\sigma/dE$) spectra or energy integrated ($d\sigma/d\Omega$) angular distributions was possible.

The goal of the present study was to gain new experimental information on the proton - gold interaction at proton energy of 2.5 GeV. Those new double differential data ($d^2\sigma/d\Omega dE$) should allow to gain deeper insight in the mechanism of non-equilibrium processes.

Details of the experimental procedure are discussed in the second section and the obtained data in the next, third section. The fourth section is devoted to model description of the measured spectra. The interpretation, summary and conclusions are presented in the last section. Formulae applied in the phenomenological parametrization are collected in the appendix.

II. EXPERIMENTAL PROCEDURE

The experiment has been performed using the internal beam of the Cooler Synchrotron COSY in the Research Center in Jülich. Due to multiple passing of the circulating internal beam through the target it was possible to achieve as high luminosity as that which can be reached only with very intensive external beam of accelerators (with the particle current of order of mA). Circulation of the beam without its immediate absorption demanded using of very thin, self supporting targets (of order of 300 μg/cm^2) what in turn resulted in negligible distortion of the reaction product spectra by interaction of the emitted particles with the target. Furthermore, during each cycle of injection and acceleration, the protons were circulating in the COSY ring slightly below the target, being slowly bumped onto the target until the beam was completely used up. Then a new cycle was started. The speed of the vertical shift of the proton beam was controlled by feedback of the observed reaction rate to avoid overloading of the data acquisition system.

The scattering chamber and the detecting system was described in detail in ref. [13]. There, however, the main interest was focused only on performance of the gridded ionization chambers which are used in the experiment for charge identification as well as for energy measurement of the reaction products by means of the Bragg curve spectroscopy. For this reason, a description of the other components of the detection system, relevant to the data discussed in the present paper, will be given here in a more detailed way.

The PISA apparatus consists of nine independent detection arms comprising various kinds of detectors. Two of these arms (placed at 15 and 120° angles in respect to the beam direction) are equipped with the Bragg curve detectors (BCD), which permit the Z-identification of the reaction products and determination of their kinetic energies with low detection energy threshold (of about 1 MeV/nucleon). The telescopes consisted of silicon detectors are installed at the detection angles of 35, 50, 80 and 100°. The detectors operate in the ultra high vacuum (UHV) of the COSY accelerator and are cooled to a temperature of -10° C. The cooling improves the energy resolution of the detectors, thus the isotopes of all ejectiles up to carbon can be identified. Due to geometrical constraints the silicon telescope detectors placed in the vacuum at 35, 50, and 80° cannot be supplied with additional detectors. Consequently light charged particles of high energies, not being stopped in the silicon detectors, cannot be detected. The upper limit of energies of particles stopped by these telescopes is about 30 - 40 MeV for protons, deuterons and tritons but increases significantly for heavier particles, e.g. for alpha particles it is around 120 MeV. Therefore these telescopes are suitable to measure the low energy part of the spectra for hydrogen isotopes, a large range of energies for helium isotopes and the full energy spectra of intermediate mass fragments. The silicon detector telescope placed at 100° in the ultra high vacuum has another construction than the telescopes mentioned above, thus it was possible to supplement it with a 7.5 cm thick CsI scintillator detector standing behind it in the air (outside the chamber), separated by a steel window of 50 μm thickness from the ultra high vacuum of COSY. At three angles (15.6, 20, and 65°), the telescopes built of silicon detectors with 7.5 cm CsI scintillator detectors standing behind them are positioned outside the chamber. The destination of these telescopes as well as that at 100° is to significantly increase range of energies of detected light charged particles and IMF's.

The particles observed at different angles in the present experiment and the energy ranges covered by the detecting system are listed in the Table I and in the Table II for isotopically identified and elementally identified ejectiles, respectively.

The absolute normalization of the data was achieved by comparison of the total cross section for ^{7}Be ejectiles extracted from angular and energy integration of the spectra measured in the present experiment with the cross section obtained from parametrization of experimental ^{7}Be production cross sections in proton-nucleus collisions, ref. [14]. Accuracy of the absolute normalization was estimated to be better than 10%.

III. EXPERIMENTAL RESULTS

In the present study the double differential spectra $d^2\sigma/d\Omega dE$ were determined for the first time for many isotopically identified intermediate mass fragments emitted from proton - gold collisions at GeV energies. This

TABLE I: Range of energies (in MeV) of isotopically identified reaction products detected at various scattering angles

Ejectile	Angle [degrees]						
	15.6	20	35	50	65	80	100
p	7.5 – 103.5	7.5 – 92.5	3.5 – 21.5	3.5 – 21.5	7.5 – 97.5	3.5 – 6.5	9.5 – 120.5
d	8.5 – 210.5	8.5 – 210.5	5.5 – 35.5	6.5 – 35.5	8.5 – 212.5	5.5 – 8.5	12.5 – 218.5
t	9.5 – 240.5	11.5 – 242.5	4.5 – 37.5	6.5 – 33.5	9.5 – 249.5	4.5 – 10.5	14.5 – 162.5
^{3}He	20.5 – 296.5	20.5 – 296.5	8.5 – 95.5	8.5 – 86.5	20.5 – 292.0	13.5 – 19.5	9.5 – 161.5
^{4}He	23.5 – 277.5	23.5 – 253.0	9.5 – 120.5	8.5 – 113.5	23.5 – 182.5	13.5 – 25.5	9.5 – 122.5
^{6}He	26.5 – 83.5	26.5 – 74.5	11.5 – 122.5	10.5 – 106.5	26.5 – 77.5	15.5 – 24.5	11.5 – 53.5
^{6}Li	43.5 – 145.5	42.5 – 147.5	17.5 – 178.0	14.5 – 178.0	41.5 – 143.5	18.5 – 48.5	18.5 – 105.5
^{7}Li	44.5 – 155.5	35.5 – 156.5	18.5 – 159.5	16.5 – 136.5	44.5 – 152.5	19.5 – 55.5	18.5 – 117.5
^{8}Li	47.5 – 113.5	47.5 – 110.5	19.5 – 115.5	17.5 – 98.5	46.5 – 112.5	21.5 – 51.5	19.5 – 85.5
^{9}Li	49.5 – 85.5	49.5 – 118.5	19.5 – 82.5	17.5 – 53.5	49.5 – 85.5	22.5 – 52.5	20.5 – 65.5
^{7}Be	61.5 – 136.5	62.5 – 146.5	24.5 – 123.5	24.5 – 138.5	61.5 – 136.5	27.5 – 69.5	27.5 – 90.5
^{9}Be	68.5 – 116.5	68.5 – 119.5	25.5 – 94.5	25.5 – 94.5	68.5 – 107.5	29.5 – 80.5	27.5 – 84.5
^{10}Be	71.5 – 116.5	71.5 – 128.5	26.5 – 101.5	23.5 – 98.5	71.5 – 122.5	30.5 – 87.5	29.5 – 80.5
^{10}B	90.5 – 123.5	92.5 – 122.5	35.5 – 92.5	30.5 – 99.5	90.5 – 111.5	38.5 – 86.5	36.5 – 90.5
^{11}B	94.5 – 136.5	94.5 – 130.5	35.5 – 116.5	31.5 – 100.5	96.5 – 114.5	39.5 – 105.5	37.5 – 91.5
^{12}B			36.5 – 96.5	35.5 –83.5		41.5 – 83.5	39.5 – 78.5

TABLE II: Range of energies (in MeV) of elementally identified reaction products detected at various scattering angles

Ejectile	Angle [degrees]					
	15	35	50	80	100	120
C	11.5 – 136.5	46.5 – 118.5	40.5 – 118.5	50.5 – 116.5	48.5 – 102.5	12.5 – 57.5
N	14.5 – 69.5	56.5 – 116.5	48.5 – 108.5	61.5 – 109.5	57.5 – 99.5	15.5 – 70.5
O	15.5 – 80.5	67.5 – 103.5	58.5 – 103.5	74.5 – 119.5	69.5 – 99.5	18.5 – 68.5
F	21.5 – 98.5					22.5 – 88.5
Ne	25.5 – 109.5					23.5 – 100.5
Na	29.5 – 127.5					26.5 – 117.5
Mg	29.5 – 106.5					28.5 – 98.5
Al	31.5 – 94.5					30.5 – 72.5

concerns ^{6}He, ^{8,9}Li, ^{7,9,10}Be, ^{10,11,12}B spectra which were not measured by Letourneau *et al.* at 2.5 GeV [11] whereas the experiment of Herbach *et al.* [10] at 1.2 GeV which detected IMF's lighter than boron had statistics allowing to extract only elemental spectra. Typical spectra for isotopically identified particles from the present experiment are shown in Fig. 1 together with data measured by Letourneau *et al.* [11]. Excellent agreement of the present data with those published by Letourneau *et al.* was achieved for all products measured in both experiments, i.e. ^{1,2,3}H, ^{3,4}He, and ^{6,7}Li. Note, that statistical errors, which are only shown for selected ^{7}Li data of Ref. [11], present indeed typical errors for all ^{7}Li data from that paper.

The energy distributions of emitted ejectiles have shapes resembling Maxwellian evaporation spectra, but because of an instrumental low-energy cutoff it was not possible to observe the maxima of these distributions for fragments heavier than boron. Although for heavier fragments the Coulomb barrier moves the position of maximum of the yield towards higher values, the large energy loss in first silicon detector of telescope prevent us from detecting heavy ejectiles at energies close to the maximum of the energy distributions. To avoid this problem, i.e. to measure low energy part of the spectra, two Bragg curve ionization chambers (BCD) were applied. They were placed at 15^0 and 120^0 scattering angles. Since BCD's allow for the identification of the charge of ejectiles only, the spectra of heavy products, i.e. C, O, N, F, Ne, Na, Mg and Al were obtained only with elemental identification. As far as we know, similar spectra were up to now investigated for the gold target only in the experiment performed at 1.0 GeV by Kotov *et al.* [17], where double differential cross sections were measured without isotopic identification.

Typical properties of the spectra, characteristic for all ejectiles, are depicted in Fig. 1. At low energy the angle independent - Maxwellian like - contribution is well visible. This isotropic energy distribution may be reproduced by the two stage model discussed below. The dashed line shown in the figure, represents predictions of this model. Another contribution, i.e. an exponential distribution, strongly varying with angle is present at higher energy in all experimental spectra. The slope of this anisotropic energy contribution increases with the angle, what may be interpreted as effect of fast motion of an emitting source in the forward direction.

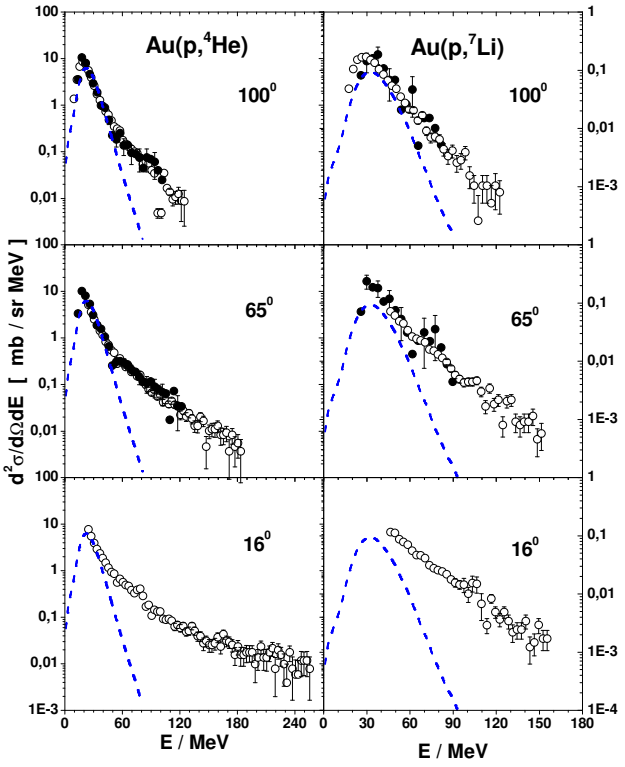

FIG. 1: Typical energy spectra of ^{4}He (left column) and ^{7}Li particles (right column) measured in the present experiment (open circles) and published in Ref. [11] (full dots) for corresponding emission angles. The lines show prediction of evaporation of ^{4}He and ^{7}Li evaluated by means of GEM program of S. Furihata [15, 16] from excited residual nuclei of the first stage of the reaction with properties extracted from BUU calculations.

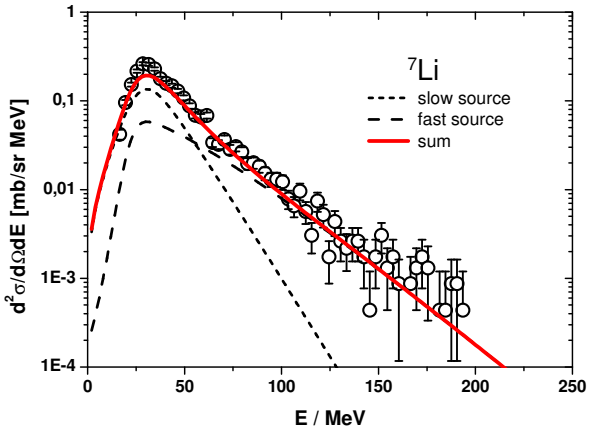

FIG. 2: Open circles represent experimental energy spectrum of ^7Li particles measured at 35^0 in the current experiment. The lines present result of phenomenological model described below; the short-dashed line shows contribution of the slow emitting source, the long-dashed line depicts contribution of the fast source, whereas the solid line presents sum of both contributions. Please note, that the shape of this experimental energy distribution as compared with spectra shown in right part of Fig. 1 also confirms the monotonic change of the exponential slope with the scattering angle.

IV. THEORETICAL ANALYSIS

In the most frequently considered scenario of the proton-nucleus collision at GeV proton energies it is assumed that reaction proceeds via two stages.

In the first stage of the reaction the proton impinging on to the target nucleus initiates a cascade of nucleon-nucleon collisions which leads to emission of several fast nucleons and pions, and to excitation of the nucleus. This fast stage of reaction is described by intranuclear cascade (INC) model, e.g. [18, 19], Boltzmann-Uehling-Uhlenbeck (BUU) model, e.g. [20] or by quantum molecular dynamics (QMD) model, e.g. [21]. The first of the mentioned models gives an account of the nucleon-nucleus interaction by static (time-independent) mean field, the BUU allows for dynamic evolution of the mean field as caused by time dependence of an average nucleon density, and the QMD treats the nucleon-nucleus interaction as a time dependent sum of elementary two-nucleon and three-nucleon interactions of all nucleons. The QMD introduces the largest fluctuations of the density distribution of nucleons and, therefore, allows for emission of clusters of nucleons from the first stage of the reaction. The static mean field description used by INC model automatically precludes possibility of nucleon distribution fluctuations. The BUU model takes into consideration a time dependent modification of the nucleon density distribution, however, the averaging over many test particles, present inherently in BUU, prohibits appearing of fluctuations large enough for nucleon clusters emission. The emission of fast nucleons (in the case of INC and BUU) or fast nucleons and light clusters (in the case of QMD) terminates after a short time, leaving the residual excited nucleus in a status close to the thermodynamic equilibrium.

The second stage of reaction consists in the evaporation of nucleons and clusters from this equilibrated system, which can also undergo fission with emission of two heavy fragments. Thus, in the two-step model of reaction mechanism, the non equilibrium emission of nucleons and clusters can appear only in the first stage of the reaction. It is believed that statistical model codes like, e.g. GEM [15, 16] or GEMINI [22] are capable to well reproduce emission of nucleons and fragments from equilibrated, excited nucleus. Therefore, observation of any disagreement of the data with predictions of the two-step model would suggest that (i) the model is not adequate to the real situation (e.g. an additional,

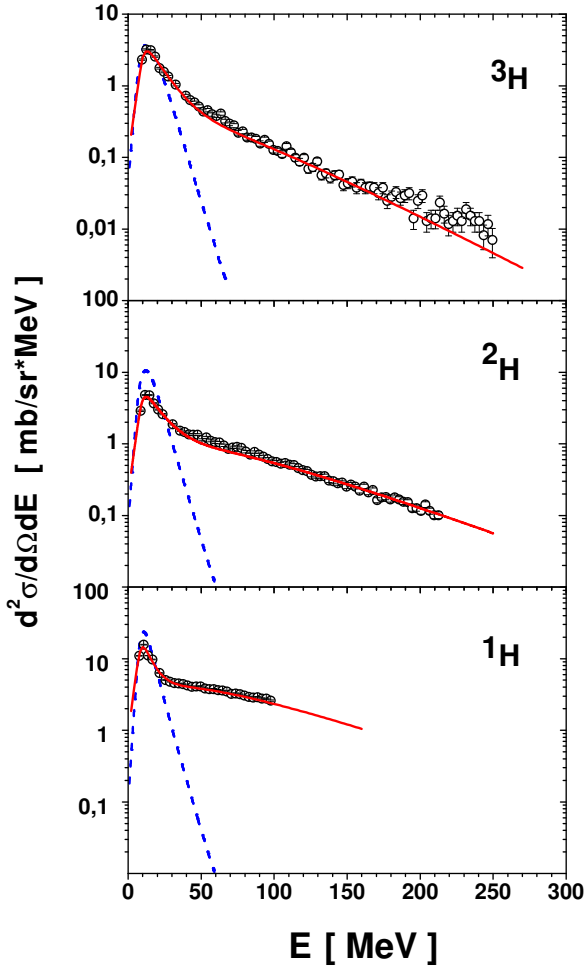

FIG. 3: Open circles represent typical spectra of protons, deuterons and tritons measured in the present experiment by telescope consisted of silicon semiconductor detectors and 7.5 cm thick scintillating detector CsI placed at scattering angle of 65 degree in respect to the proton beam. The dashed lines show evaporation contribution evaluated by means of the BUU and Generalized Evaporation Model whereas the full lines correspond to phenomenological model of two emitting sources described below. Note change of the scale for the triton spectrum.

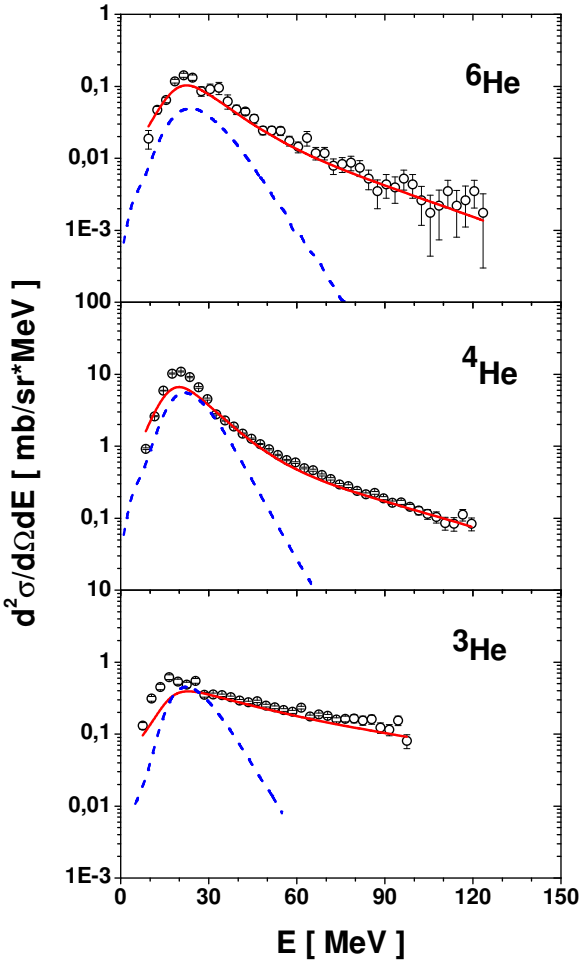

FIG. 4: Typical energy spectra of helium ions ^{3,4,6}He measured in the present experiment by telescope consisted of silicon semiconductor detectors placed at scattering angle of 35 degree in respect to the proton beam - open circles. Note different vertical scales for each spectrum. The lines have the same meaning as in Fig. 3

intermediate stage of the process is necessary before achieving thermodynamic equilibrium), or (ii) description of the emission of particles from the first stage of the reaction (nucleons or clusters) is not properly taken into consideration.

A. Boltzmann-Uehling-Uhlenbeck model and evaporation model

The present data were compared with results of a two stage model in which the Boltzmann-Uehling-Uhlenbeck transport equation [20] has been applied for the description of the first step of the proton - nucleus collision leading to emission of fast nucleons leaving the heavy excited remnant in a state close to equilibrium. Monte Carlo computer program developed at Giessen University [23] was utilized to simulate this first stage of the reaction and to find properties of excited residual nuclei. Deexcitation of these nuclei, which proceeds by emission of nucleons and complex fragments, was calculated in

the frame of statistical model using the GEM (Generalized Evaporation Model) computer program of Furihata [15, 16]. Theoretical energy spectra of various ejectiles found from this two stage model are shown in Figs. 1 - 8 as dashed lines. It can be concluded from examination of these figures that the model predictions describe well low energy part of spectra for hydrogen, helium and lithium isotopes. For heavier ejectiles the theoretical cross sections underestimate the experimental data. Moreover, it can be observed that the high energy part of the spectra is clearly not reproduced by the two stage model, which predicts much steeper slope of the spectra than is observed experimentally. Thus, another mechanism seems to give a significant contribution to the proton - nucleus reactions. As concerns hydrogen and helium production, the authors of [10], [11], and [12] papers propose the coalescence of nucleons as the mechanism responsible for this effect, however, no microscopic model is able to reproduce observed effects for heavier composite ejectiles.

An extensive comparison of predictions resulting from the models mentioned above with our experimental data presented here will be subject of a forthcoming paper. We restrict ourselves here on conclusions we can draw from the application of a phenomenological model described in the next section.

Following properties of the spectra should be taken into consideration when looking for an appropriate phenomenological model:

(i) The position of the peak present at low energies in the experimental spectra of all observed particles (and its height for light ejectiles) is quite well reproduced by the two stage model discussed above. This means that the mechanism described by this model gives a large contribution to the reaction and therefore it must be taken into account in the frame of any phenomenological model.

(ii) The slope of the exponential, high energy tail of the experimental spectra for all ejectiles varies monotonically, increasing strongly with the scattering angle as can be seen from Fig. 1. Such a behavior is in contradistinction to properties of the spectra evaluated in the frame of the two stage model, which are almost independent of angle. This indicates that high energy particles are not emitted from heavy residuum of the intranuclear cascade but from another source which moves much faster than the residuum.

These arguments call for using of a phenomenological model of two emitting sources; one source moving slowly would imitate emission from heavy residuum of the intranuclear cascade whereas the second source should simulate emission from faster (and thus probably lighter) nuclear system. Of course, one could imagine that more than two sources of emitted particles are necessary for reasonable description of the data. The applied model of two moving sources corresponds to minimal number of parameters necessary to fulfill qualitative demands put on the model by the experimental data.

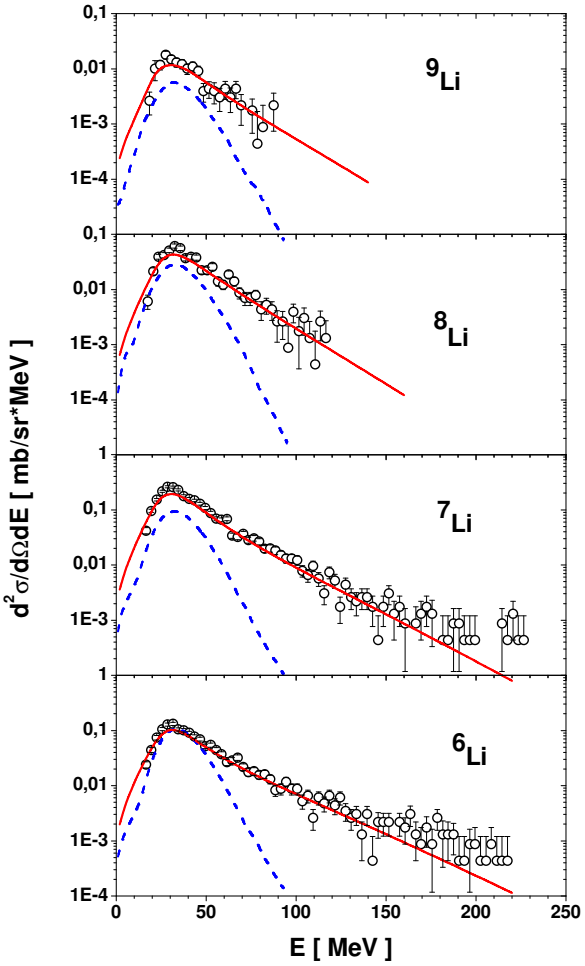

FIG. 5: Typical spectra of lithium ions ^{6,7,8,9}Li measured in the present experiment by telescope consisted of silicon semiconductor detectors placed at scattering angle of 35 degree in respect to the proton beam - open circles. Note different vertical scales for ^{6,7}Li and ^{8,9}Li. The lines have the same meaning as in Fig. 3

B. Phenomenological model of two moving sources

In the frame of the phenomenological model of two moving sources the angular and energy dependence of the double differential cross sections $d^2\sigma/d\Omega dE$ is described by analytical formulae. The details of the model and interpretation of its parameters are presented in the Appendix. An example of the description of the experimental energy spectrum by the two source model is shown in Fig. 2. The symbols depict the data from present ex-

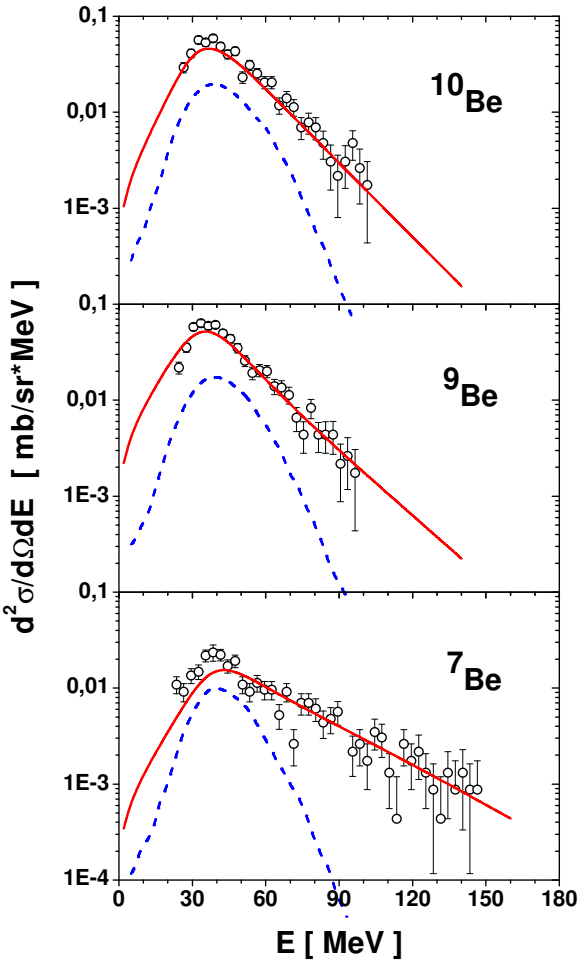

FIG. 6: Typical spectra of beryllium ions ^{7,9,10}Be measured in the present experiment by telescope consisted of silicon semiconductor detectors placed at scattering angle of 35 degree in respect to the proton beam - open circles. The lines have the same meaning as in Fig. 3

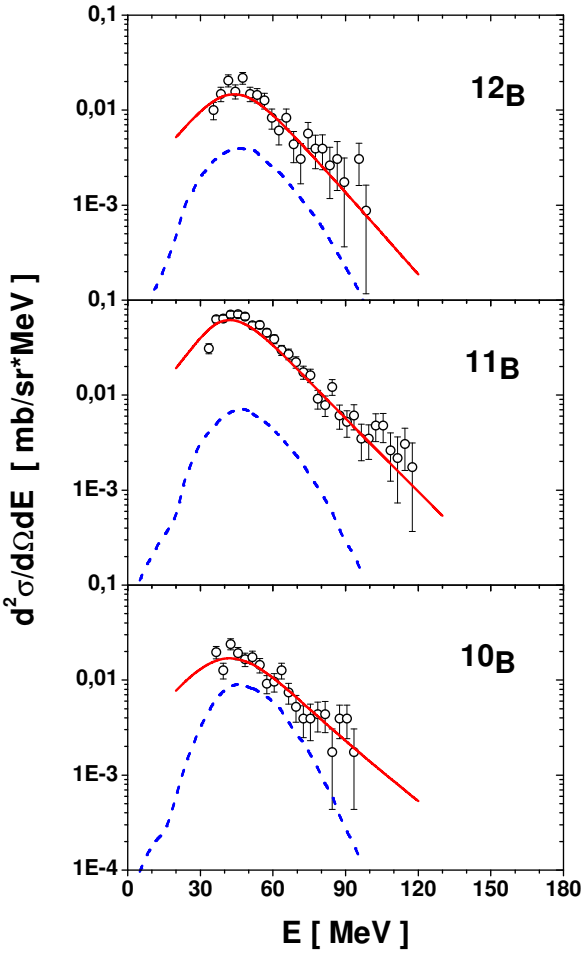

FIG. 7: Typical spectra of boron ions ^{10,11,12}B measured in the present experiment by telescope consisted of silicon semiconductor detectors placed at scattering angle of 35 degree in respect to the proton beam - open circles. The lines have the same meaning as in Fig. 3

periment obtained for ^{7}Li ejectiles detected at scattering angle 35^0 whereas the lines show result of the fit of the phenomenological model. The short-dashed line presents contribution from the slowly moving source, the long-dashed line shows contribution from the fast source and the solid line corresponds to sum of both contributions. As can be seen, very good description of full energy spectrum could be achieved.

The parameters of the theoretical formula of the two moving sources model have been searched for by fitting simultaneously experimental spectra at several scattering angles for each ejectile. Exceptions from this rule were the spectra of ejectiles heavier than oxygen (F, Ne, Na, Mg, and Al), which were measured only at these two angles at which Bragg curve ionization chambers have been positioned, *i.e.* at 15^0 and 120^0. Such spectra were fitted assuming that only one moving source gives contribution to the reaction. Furthermore, the spectra of C, N, and O which were measured both, by silicon detectors at 35^0, 50^0, 80^0, and 100^0 as well as by Bragg curve ionization chambers at 15^0 and 120^0 degree were fitted using one emitting source and two emitting sources. The parameters of sources for light charged particles and isotopically identified IMF's are listed in Table III whereas those for heavier IMF's, which were only elementally identified, are collected in Table IV.

The first source should simulate evaporation of particles from heavy remnant of the first stage of the reaction, *i.e.* intranuclear cascade of nucleon-nucleon collisions. Thus, its velocity was fixed at value β=0.002

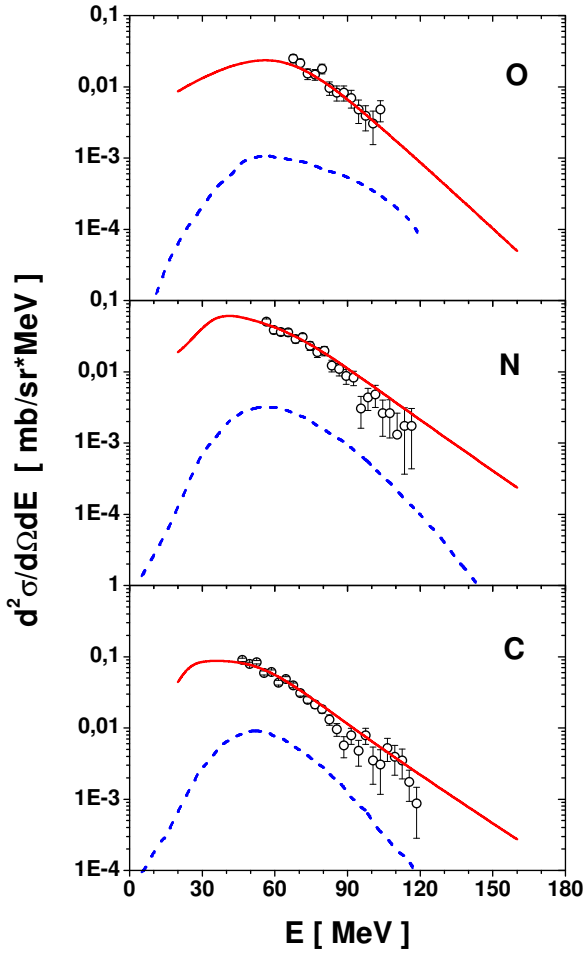

FIG. 8: Typical spectra of carbon, nitrogen and oxygen ions measured in the present experiment without isotopic separation by telescope consisted of silicon semiconductor detectors placed at scattering angle of 35 degree in respect to the proton beam - open circles. The lines have the same meaning as in Fig. 3

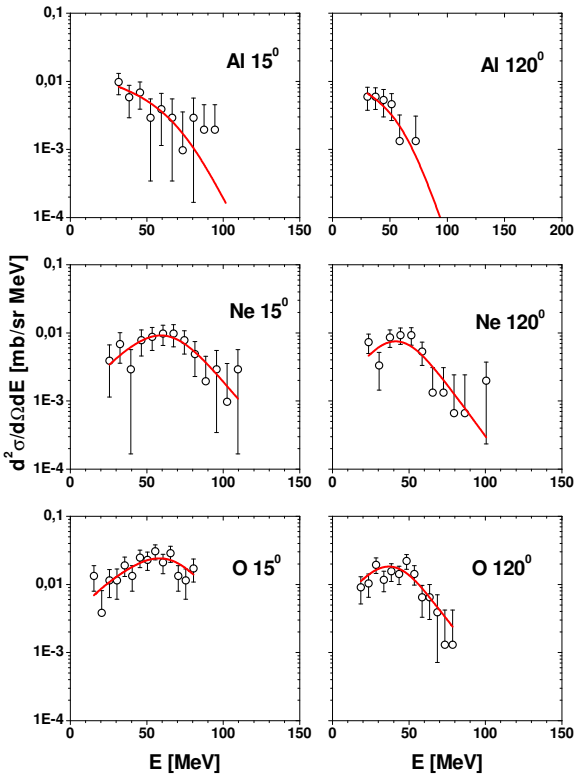

FIG. 9: Examples of energy spectra for heavier, elementally identified IMF's obtained in the current experiment by means of Bragg curve ionization chambers. The open circles represent experimental data and the solid lines show results of phenomenological model analysis obtained with assumption of only one moving source, discussed in the next section of the paper.

(in units of velocity of light) as it was extracted from BUU calculations. This value was constant for all calculations. Other parameters characterizing the source, *i.e.* k-parameter (ratio of the actual height of Coulomb barrier to its value found from simple estimation for two touching, charged spheres), T-parameter (apparent temperature), and σ (energy and angle integrated cross section for production of given ejectile) were free parameters of the fit.

All parameters of the second source were freely modified in fits since no hypothesis concerning origin of this source was made before the analysis. Usually the program was able to find unambiguously the best parameters, corresponding to the minimum value of chi-square. In such a situation the routine provides estimation of errors. In some cases, however, the valley of chi-square values was so complicated that the program was not able to produce reasonable estimation of errors. The ambiguity of parameters lead sometimes the searching procedure to nonphysical values of the parameters, as *e.g.* negative height of the Coulomb barrier. Then it was necessary to fix these parameters at values, which still have physical meaning. Such values of parameters are quoted in the tables as closed in square parentheses.

Thorough inspection of the parameter dependence leads to the following conclusions:

1. ***The contribution σ_1 of the first (slow) emitting source is comparable to contribution σ_2 of the second source.***

   It is illustrated by Fig. 10 in which ratio of the total cross section for emission of ejectiles from the first source to the sum of the total cross sections for emission from both sources is shown as function of mass number of the ejectiles. The average value of

TABLE III: Parameters of two moving sources for isotopically identified products

Ejectile	Slow source			Fast source				χ^2
	k_1	T_1/MeV	σ_1/mb	k_2	β_2	T_2/MeV	σ_2/mb	
p	0.67 ± 0.02	5.6 ± 0.3	1712 ± 46	[0.05]	0.147 ± 0.005	51.0 ± 1.4	4839 ± 86	22.6
d	0.75 ± 0.02	9.2 ± 0.4	870 ± 29	0.07 ± 0.01	0.127 ± 0.004	48.3 ± 0.8	1100 ± 24	13.2
t	0.85 ± 0.02	9.5 ± 0.3	627 ± 17	[0.05]	0.072 ± 0.003	36.1 ± 0.7	323 ± 13	6.1
^{3}He	0.75 ± 0.03	14.9 ± 0.8	112 ± 7	[0.05]	0.083 ± 0.005	45.5 ± 1.2	106 ± 7	4.6
^{4}He	0.82 ± 0.02	7.8 ± 0.3	1722 ± 43	0.30 ± 0.09	0.048 ± 0.005	26.6 ± 1.5	251 ± 30	59
^{6}He	0.97 ± 0.04	9.0 ± 0.6	24.8 ± 1.4	0.35 ± 0.05	0.040 ± 0.007	21.6 ± 1.4	7.5 ± 1.4	2.1
^{6}Li	0.86 ± 0.04	11.1 ± 0.8	25.3 ± 1.7	0.44 ± 0.04	0.034 ± 0.003	23.7 ± 0.6	14.5 ± 1.7	2.0
^{7}Li	0.88 ± 0.03	11.6 ± 0.6	50.8 ± 2.6	0.36 ± 0.03	0.035 ± 0.003	20.9 ± 0.5	20.3 ± 2.6	3.1
^{8}Li	0.90 ± 0.09	11.9 ± 1.5	9.1 ± 1.4	0.45 ± 0.05	0.029 ± 0.005	18.0 ± 1.0	6.4 ± 1.5	2.1
^{9}Li	1.00 ± 0.22	10.4 ± 3.0	2.1 ± 0.5	0.39 ± 0.07	0.025 ± 0.003	18.2 ± 1.6	2.1 ± 0.6	1.2
^{7}Be	0.92 ± 0.27	11.2 ± 4.3	2.6 ± 0.8	0.48 ± 0.05	0.038 ± 0.005	24.0 ± 1.2	4.6 ± 0.9	1.4
^{9}Be	0.86 ± 0.12	9.6 ± 1.7	12.5 ± 1.9	0.53 ± 0.06	0.020 ± 0.005	16.6 ± 0.8	8.1 ± 2.3	1.4
^{10}Be	0.90 ± 0.08	11.8 ± 1.2	10.0 ± 1.4	0.44 ± 0.04	0.026 ± 0.004	14.5 ± 0.9	6.8 ± 1.5	1.3
^{10}B	0.85 ± 0.20	10.5 ± 3.4	6.6 ± 1.3	0.73 ± 0.14	0.020 ± 0.010	18.2 ± 2.7	2.7 ± 1.7	1.8
^{11}B	0.93 ± 0.18	10.5 ± 2.1	12.8 ± 2.5	0.50 ± 0.05	0.022 ± 0.004	14.5 ± 0.7	12.8 ± 2.8	1.7
^{12}B	0.87	8.8	1.6	0.73	0.012	13.2	5.1	1.0

TABLE IV: Parameters of one or two moving sources for elementally identified products

Ejectile	Slow source			Fast source				χ^2
	k_1	T_1/MeV	σ_1/mb	k_2	β_2	T_2/MeV	σ_2/mb	
C	0.879	12.3	28.4	0.150	0.0367	15.8	11.8	3.34
				0.759 ± 0.032	0.0076 ± 0.0007	13.4 ± 0.5	33.4 ± 0.9	3.26
N	1.00	12.2	15.9	0.206	0.0382	14.5	9.6	1.47
				0.822 ± 0.045	0.0118 ± 0.0007	13.4 ± 0.6	18.6 ± 0.7	1.41
O	0.75	14.1	1.3	0.71	0.0129	12.2	11.8	0.78
				0.784 ± 0.045	0.0118 ± 0.0007	13.5 ± 0.6	13.1 ± 0.6	0.75
F				0.545 ± 0.079	0.0105 ± 0.0014	17.0 ± 3.2	5.12 ± 0.32	0.40
Ne				0.670 ± 0.098	0.0090 ± 0.0018	15.3 ± 1.9	5.25 ± 0.44	0.54
Na				0.801 ± 0.117	0.0104 ± 0.0020	12.0 ± 0.7	5.99 ± 0.63	0.61
Mg				0.577 ± 0.090	0.0103 ± 0.0019	12.0 ± 1.2	4.59 ± 0.52	0.59
Al				0.772 ± 0.180	0.0036 ± 0.0013	10.0 ± 0.7	5.24 ± 0.91	0.23

the ratio $\sigma_1/(\sigma_1+\sigma_2)$ is equal to 0.560 ± 0.044. It should be, however, emphasized that rather large deviations from the average value appear for individual ejectiles. For example, almost 90 % of alpha particles is emitted from the slow source, whereas it is the case only for ~ 25 % of protons.

2. ***The parameters of the slow source have values which agree with the assumption that this source simulates evaporation from a heavy nucleus*** corresponding, *e.g.* to the residuum of the target after the intranuclear cascade of nucleon-nucleon collisions, namely:

   - The apparent temperature of the slow source is independent of the mass of emitted intermediate mass fragments, what can be seen in Fig. 11 where the slope parameter of the solid line is equal to zero within the limits of errors : - 0.15 ± 0.17. Its stability indicates that the recoil effect of the source during emission of fragments is negligible, thus, mass of the source must be much larger than masses of observed IMF's (cf. Appendix). Moreover, the horizontal line: $T = 11.9 \pm 1.5$ MeV, fitted to temperature values extracted from spectra of IMF's reproduces also quite well values of the apparent temperature for light charged particles (H and He ions) as can be expected for emission from heavy residuum of the intranuclear cascade of nucleon-nucleon collisions.

   - The k parameter, which determines the height of the effective Coulomb barrier between the emitted fragment and the rest of the emitting source (cf. Appendix) is very close to unity, what means that the charge of the source does not differ significantly from the charge of the target. It is illustrated by Fig. 12 where k parameters for both sources are shown for individual ejectiles. The full squares represent the slow source and open squares correspond to the second, fast source. The dashed line $k = 1$ is shown in the figure to facilitate judg-

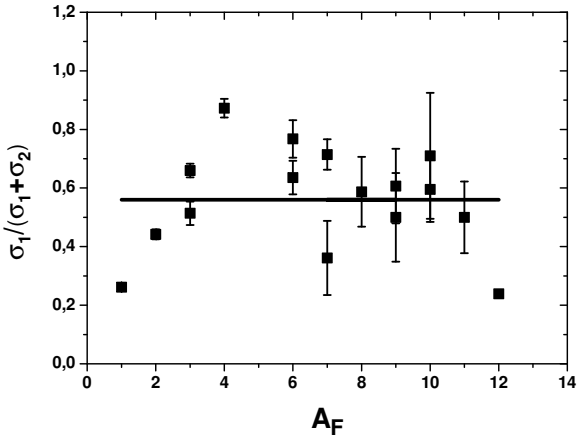

FIG. 10: Ratio of total production cross section corresponding to emission from the slow source to sum of the total cross sections representing emission from both sources versus mass number of the detected reaction product. The parameters σ_1 and σ_2 were taken as total cross sections because they correspond to angle and energy integrated double differential cross sections $d^2\sigma/d\Omega dE$. The solid line shows average value of the ratio (0.560 ± 0.044).

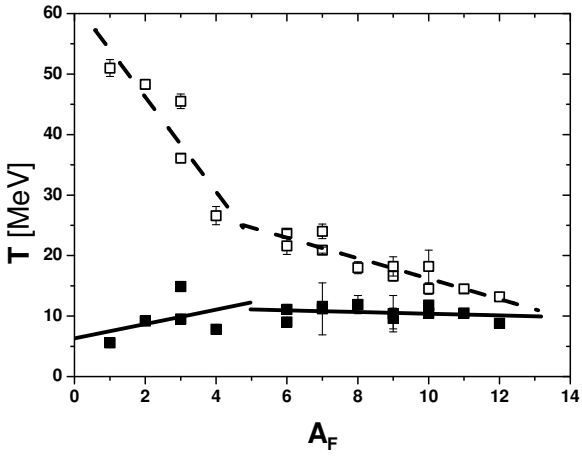

FIG. 11: Apparent temperature of the slow source (full squares and solid lines) and that of the fast source (open squares and dashed lines) versus mass number of the ejectiles. The lines were fitted separately for light charged particles (^{1}H - ^{4}He) and intermediate mass fragments ($A_F \geq 6$).

ment on the magnitude of the k – parameter.

3. ***The second (fast) source is much lighter than the residual nucleus of the intranuclear cascade*** because:

   - Its velocity is always larger than limiting velocity of the proton-target center of mass which would be obtained only when total beam momentum is transferred to the target ($\beta \approx 0.018$). Fig. 13 illustrates this fact showing β_2 values for individual ejectiles as well as the horizontal line $\beta = 0.018$.
   - The Coulomb barrier between the source and the ejectile is several times smaller than the Coulomb barrier of two touching charged spheres representing the target nucleus and the ejectile. This is well illustrated by open squares in Fig. 12.
   - The recoil effect (cf. Appendix) is clearly visible in the dependence of the apparent temperature of the source on the mass of the ejectile as it is shown in Fig. 11 - open squares.

4. ***The fast source describing LCP's emission (hydrogen and helium ions up to ^{4}He) is much lighter than the fast source responsible for emission of intermediate mass fragments.***

   This may be inferred from different recoil effects visible as different slopes of two lines which describe the dependence of the apparent temperature on the mass of ejectiles (cf. Fig. 11). The line corresponding to LCP's is more steep, giving the mass of the source equal to A_S=(8 ± 2) nucleons, and very high temperature of the source τ=(62 ± 7) MeV (cf. Appendix for meaning of τ). Velocity of this light source is very high; $\beta = 0.05 - 0.15$. Such a source can be, perhaps, identified with the *fireball* created by the proton impinging on to the target together with nucleons present on its straight line way through the target nucleus [24],

   The line describing temperature of IMF's corresponds to mass of the source A_S=(20 ± 3) nucleons and its temperature τ= (33 ± 2) MeV. Velocity of this source is much smaller ($\beta = 0.02 - 0.04$) than velocity of source emitting LCP's.

Very different properties of the fast source emitting light charged particles (LCP's) and the fast source emitting intermediate mass fragments (IMF's) leads to conclusion that the picture of two sources is oversimplified. The presence of a fireball, which can give contribution to emission of LCP's only and occurrence of the light ($A_S \approx 20$), fast source emitting LCP's as well as IMF's may be interpreted as indication of a three body decay of the target nucleus. The third partner of such a decay would be heavy and hardly distinguishable from heavy residuum of the intranuclear cascade, therefore its occurrence could be described effectively by the same slow source.

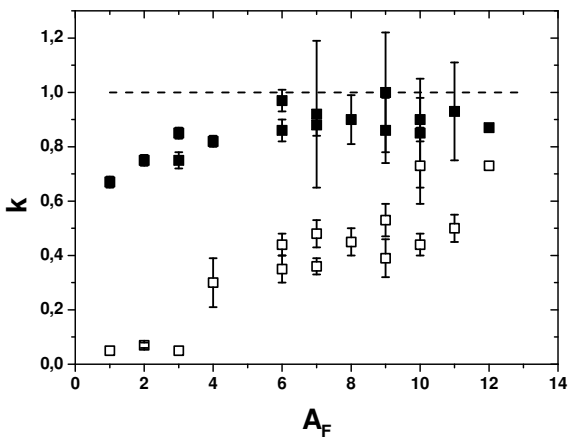

FIG. 12: The ejectile mass number dependence of the factor scaling the Coulomb barrier of two touching spheres to the actual height – necessary for good description of the data. Full squares represent the slow source and open squares show results for the fast source. The line k=1 is also depicted to facilitate interpretation of the figure.

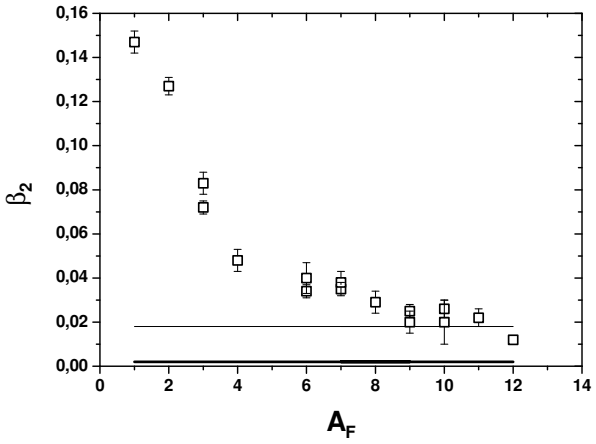

FIG. 13: Velocity of the second (fast) source as a function of emitted fragment mass number - open squares. Thin solid line β_2=0.018 represents velocity of the common center of mass of the proton projectile and the target and thick solid line β_1=0.002 shows velocity of the first (slow) source fixed at velocity of heavy residuum of intranuclear cascade.

V. SUMMARY AND CONCLUSIONS

The double differential cross sections ($d^2\sigma/d\Omega dE$) were for the first time measured with good statistics for isotopically identified intermediate mass fragments produced by interaction of 2.5-GeV protons with the gold target. The following individual isotopes of the elements from hydrogen to boron were resolved: ^{1,2,3}H, ^{3,4,6}He, ^{6,7,8,9}Li, ^{7,9,10}Be, ^{10,11,12}B, whereas for heavier ejectiles (from carbon to aluminium) only elemental identification was done. The energy spectra for all nuclear fragments, determined at several scattering angles, appear to be of the Maxwellian shape with exponential, high energy tail. The low energy part of the distribution is almost independent of angle, but the slope of high energy tail of the spectrum increases monotonically with the angle. The shape of the angle independent part of spectra can be reproduced by the two-stage model of the reaction, i.e. intranuclear cascade of the nucleon-nucleon and meson-nucleon collisions followed by statistical emission from an equilibrated residual nucleus. However, the absolute magnitude of the spectra predicted by two-stage model, using Boltzmann-Uehling-Uhlenbeck program [23] for the intranuclear cascade and Generalized-Evaporation-Model (GEM) [15, 16] for statistical emission of fragments, is in agreement with the experimental data only for the light charged particles (H and He ions). Furthermore, the theoretical cross sections underestimate significantly the yield of heavier fragments at high kinetic energies for all ejectiles. This indicates that another mechanism plays an important role besides the standard two-stage mechanism.

To get information on possible origin of this additional mechanism a phenomenological analysis was performed assuming that the ejectiles originate from two moving sources. The slow moving source was identified with the heavy remnant nucleus of the first stage of the two-step process mentioned above while no assumptions have been made as concerns the second emitting source. The properties of both sources were treated as free parameters with exception of the velocity of the slow source which was taken to be equal to the velocity of the heavy residual nucleus from the intranuclear cascade, namely β_1=0.002.

Excellent agreement of the phenomenological parametrization with experimental data was achieved with values of the parameters varying smoothly from ejectile to ejectile. Their behavior indicates that the parameters of the slow source are compatible with the assumption that it is a heavy nucleus which may be described as equilibrated system of $\sim$ 12 MeV apparent temperature, whereas the second source has completely different properties. It corresponds either to very small ($A_S \sim 8$), very hot ($\tau \sim 62$ MeV) and fast ($\beta = 0.05 - 0.15$) fireball or to heavier ($A_S \sim 20$), colder ($\tau \sim 33$ MeV), and slower ($\beta = 0.02 - 0.04$) cluster.

The described above properties of two emitting sources observed in the interaction of 2.5 GeV protons

with the gold target lead to a conclusion that two different mechanisms are observed giving almost the same contribution to the cross sections. First of them is compatible with the standard, two-stage model whereas another one seems to be similar to the picture of cold break-up proposed by J. Aichelin, J.Hüfner and R. Ibarra [25].

In the model of cold break-up the energetic proton bombarding the target drills a cylindrical hole through the nucleus causing that the deformed remnant of the collision breaks up into two pieces. Thus, three correlated groups of nucleons appear after first, short stage of the reaction : (i) the fast, small cluster consisted of the nucleons which were placed within the cylinder with the axis along to the projectile path,(ii) two clusters - products of the break up. All three clusters act as sources emitting light charged particles, whereas two heavier clusters are also responsible for emission of intermediate mass fragments. The two latter clusters are produced in result of a dynamical process in which the "wounded" nucleus cannot come to its ground state by emission of nucleons or small clusters, however, the correlation of the fast group of nucleons knocked out by the projectile is of another, kinematic origin. The high energy proton impinging on to the nucleus sees it - due to Lorentz contraction - as a narrow disc. Therefore all the nucleons which lie on the path of the projectile interact simultaneously, as one entity, with the projectile. It was shown that this collectivity affects the multi particle production in proton-nucleus collisions [26] as well as manifests itself in enhanced dependence of momentum transfer on projectile energy in deep-spallation reactions [27]. Thus, it is not surprising that such correlated group of nucleons can appear as a hot, fast moving source emitting light charged particles observed in the present experiment. Of course, it cannot give contribution to emission of intermediate mass fragments because the source is consisted of a few nucleons only.

It might be something confusing why in the present parametrization only two sources were necessary for good description of the data if the postulated cold break-up mechanism of the reaction calls for presence of three sources. This apparent inconsistency is easy to be removed: The slow, heavy source represents the heavy residual nucleus produced by the standard two-step model of the reaction and/or the heavy fragment from the break up . The light, fast source is responsible for simulation of the hot fireball (for light charged particles) or the lighter fragment from the break up (for intermediate mass fragments).

Consistency of the present phenomenological description with the cold break up picture of the reaction cannot be assumed as a proof of the underlying reaction mechanism. Additional experimental facts should be searched for establishing the confidence in such an interpretation. For example, it can be expected that similar phenomena have to appear for other heavy target nuclei if they are observed for the gold target. On the contrary, it is not obvious whether proton induced reactions on light targets or at significantly different proton energies should show similar behavior.

APPENDIX: PHENOMENOLOGICAL PARAMETRIZATION

In this Appendix assumptions and details of the formulation of two moving source model are discussed. The content of the appendix is very close to information contained in the original paper of Westfall *et al.* [28], however, the additional modification and properties introduced in the model need to be discussed for proper understanding of the performed analysis.

The model assumes that the nucleons and composite particles are emitted from two moving sources with the following properties:

(i) Each source moves along the proton beam direction,

(ii) Angular distribution of emitted particles is isotropic in the source rest frame,

(iii) Distribution of the kinetic energy E^* available in the two-body break up of the source has a Maxwellian shape characterized by the temperature parameter τ:

$$\frac{d^2\sigma}{dE^* d\Omega^*} = \frac{\sigma}{2\left(\pi\tau\right)^{3/2}}\sqrt{E^*}\exp\left[-\frac{E^*}{\tau}\right].$$

The distribution is normalized in such a way that integration over angles and energies gives the total cross section equal to the parameter σ.

Since the mass of the source A_S is finite, the energy and momentum conservation laws cause that the energy $E^{'}$ of the observed particle of mass A_F differs from the full kinetic energy E^* available in the source frame:

$$E^* = \nu E^{'} \quad \text{where} \quad \nu \equiv \frac{A_S}{A_S - A_F},$$

thus the energy distribution of the emitted fragment in the rest frame of the source is given by:

$$\frac{d^2\sigma}{dE' d\Omega'} = \frac{\nu\sigma}{2\left(\pi\tau\right)^{3/2}}\sqrt{\nu E'}\exp\left[-\frac{\nu E^{'}}{\tau}\right].$$

This formula is usually applied without explicit writing the recoil correction, i.e. by introducing so called *apparent temperature* $T \equiv \tau/\nu$:

$$\frac{d^2\sigma}{dE' d\Omega'} = \frac{\sigma}{2\left(\pi T\right)^{3/2}}\sqrt{E'}\exp\left[-\frac{E^{'}}{T}\right].$$

Such a form of this formula is used also in the present paper.

It is worth to note, that the recoil of the source gives a possibility to extract the information on the source temperature parameter τ as well as on the mass of the source A_S from linear dependence of the apparent temperature T on the fragment mass A_F:

$$T \equiv \frac{\tau}{\nu} = \tau - \left(\frac{\tau}{A_S}\right) \cdot A_F \ .$$

The charged particles emitted from the source must overcome the Coulomb barrier, what significantly changes the shape of the low energy part of their spectrum. The presence of the barrier may be taken into account by shifting the argument in the Maxwell formula by the height of the barrier, as it was originally proposed in Ref. [28] or by multiplying the Maxwell distribution by the transmission factor. The first method is equivalent to the application of a sharp cut-off what is a too crude approximation, thus the result must be averaged over some distribution of heights of the barriers [28]. The second method explicitly introduces a smooth variation of the transition probability with energy, however, this method also must introduce some assumptions concerning height and curvature of the barrier. In the present work, the probability P to overcome the Coulomb barrier was parameterized in the following form:

$$P = \frac{1}{1 + \exp\left[-\left(\frac{E - k\cdot B}{d}\right)\right]} \ ,$$

where B is the Coulomb barrier of two touching spheres corresponding to the emitted fragment of mass number A_F and charge number Z_F and to the remaining part of the source with the mass number of $(A_S - A_F)$ and charge number $(Z_S - Z_F)$:

$$B = \frac{Z_F(Z_S - Z_F)e^2}{1.44\left({A_F}^{1/3} + (A_S - A_F)^{1/3}\right)} \ .$$

The quantities k and d are the parameters. The first parameter (k) gives magnitude of the Coulomb barrier in units of B. To avoid ambiguity of B determination arising from the fact that at least two different sources are present in the current analysis, we evaluated B value assuming that $Z_S = 79$ and $A_S = 197$, *i.e.* there are atomic and mass numbers of the target. Such value of B is a good approximation of the Coulomb barrier for heavy residua of the intranuclear cascade, thus one should expect that then the k parameter is close to unity. However, with such definition of B, the k parameter should be significantly smaller than unity for light sources. The parameter k was searched by looking for the best fit of model spectra to the experimental data. The second parameter (d) was arbitrarily fixed in the present analysis by keeping constant the ratio of the height of the barrier kB to its diffuseness parameter d: $kB/d = 5.5$.

The explicit introduction of the barrier penetration factor P gives finally the following formula for the double differential cross section $d^2\sigma/dE^{'}d\Omega^{'}$:

$$\frac{d^2\sigma}{dE'\,d\Omega'} = \frac{\sigma}{4\pi T^{3/2} I(kB,d,T)} \cdot \frac{\sqrt{E'}\exp\left(-\frac{E^{'}}{T}\right)}{1+\exp\left(\frac{kB-E'}{d}\right)}$$

$$I(B,d,T) = \int_0^\infty \frac{dx\cdot\sqrt{x}\cdot\exp(-x)}{1+\exp\left(\frac{kB-T\cdot x}{d}\right)}$$

The integral $I(B,d,T)$ used for normalization of the distribution (preserving previous interpretation of σ parameter) has been evaluated numerically by the Gauss-Laguerre method.

It is necessary to transform the model double differential cross sections calculated in the rest frame of the emitting source to the laboratory system when comparing the model predictions to experimental data. It can be shown that the transformation may be performed by following formula:

$$\frac{d^2\sigma}{dEd\Omega} = \frac{p}{p'}\cdot\frac{d^2\sigma}{dE'd\Omega'} \approx \sqrt{\frac{E}{E'}}\cdot\frac{d^2\sigma}{dE'd\Omega'} \ ,$$

where the first equality is exact and the second is valid in nonrelativistic limit, normally realized in the motion of observed ejectiles. The nonrelativistic relationship between kinetic energy E of the particle emitted at the angle θ_{LAB} in the laboratory system and the energy $E^{'}$ of emitted particle in the rest frame of the source is as follows:

$$E^{'} = E + \frac{m\beta^2}{2} - \sqrt{2mE}\cdot\beta\cdot\cos\theta_{LAB} \ ,$$

where m $(\equiv A_F)$ is the mass of the emitted particle and β - the velocity of the source in the laboratory system.

ACKNOWLEDGMENTS

The quality of the beam necessary for the success of this work is due mainly to the efforts of the COSY operator crew. The authors acknowledge gratefully the support of the European Community-Research Infrastructure Activity under FP6 "Structuring the European Research Area" programme (CARE-BENE, contract number RII3-CT-2003-506395 and HadronPhysics, contract number RII3-CT-2004-506078). The authors appreciate the financial support of the European Commission through the FP6 IP-EUROTRANS FI6W-CT-2004-516520.

[1] S. Kaufman and E. Steinberg, Phys. Rev. C **22**, 167 (1980).

[2] Y. Asano, H. Kariya, S. Mori, M. Okano, and M.Sakano, J. Phys. Soc. Japan **57**, 2995 (1988).

[3] M. Cherry, A. Dąbrowska, P. Deines-Jones, R. Hołyński, W. Jones, E. Kolganova, A. Olszewski, K. Sengupta, T. Skorodko, M. Szarska, et al., Phys. Rev. C **52**, 2652 (1995).

[4] C. J. Waddington, J. R. Cummings, B. S. Nilsen, and T. L. Garrard, Phys. Rev. C **61**, 024910 (2000).

[5] F. Rejmund, B. Mustapha, P. Armbruster, J. Benlliure, M. Bernas, A. Boudard, J. Dufour, T. Enqvist, R. L. S. Leray, K.-H. Schmidt, et al., Nucl. Phys. A **683**, 540 (2001).

[6] J. Benlliure, P. Armbruster, M. Bernas, A. Boudard, T. Enqvist, R. Legrain, S. Leray, F. Rejmund, K.-H. Schmidt, C. Stéphan, et al., Nucl. Phys. A **700**, 469 (2002).

[7] M. K. Berkenbusch, W. Bauer, K. Dillman, S. Pratt, L. Beaulieu, K. Kwiatkowski, T. Lefort, W. c. Hsi, V. E. Viola, S. J. Yennello, et al., Phys. Rev. Lett. **88**, 022701 (2002).

[8] V. Rodionov, S. Avdeyev, V. Karnaukhov, L. Petrova, V. Kirakosyan, P. Rukoyatkina, H. Oeschler, A. Budzanowski, W. Karcz, M. Janicki, et al., Nucl. Phys. A **700**, 457 (2002).

[9] V. Karnaukhov, H. Oeschler, S. Avdeyev, E. Duginova, V. Rodionov, A. Budzanowski, W. Karcz, O. Bochkarev, E. Kuzmin, L. Chulkov, et al., Phys. Rev. C **67**, 011601(R) (2003).

[10] C. M. Herbach, D. Hilscher, U. Jahnke, V. G. Tishchenko, J. Galin, A. Letourneau, A. Péghaire, D. Filges, F. Goldenbaum, L. Pieńkowski, et al., Nucl. Phys. A **765**, 426 (2006).

[11] A. Letourneau, A. Böhm, J. Galin, B. Lott, A. Péghaire, M. Enke, C.-M. Herbach, D. Hilscher, U. Jahnke, V. Tishchenko, et al., Nucl. Phys. A **712**, 133 (2002).

[12] A. Boudard, J. Cugnon, S. Leray, and C. Volant, Nucl. Phys. A **740**, 195 (2004).

[13] R. Barna, V. Bollini, A. Bubak, A. Budzanowski, D. D. Pasquale, D. Filges, S. V. Förtsch, F. Goldenbaum, A. Heczko, H. Hodde, et al., Nucl. Instr. Meth. in Phys. Research A **519**, 610 (2004).

[14] A. Bubak, B. Kamys, M. Kistryn, and B. Piskor-Ignatowicz, Nucl. Instr. and Meth. in Phys. Research B **204**, 507 (2004).

[15] S. Furihata, Nucl. Instr. and Meth. in Phys. Research B **71**, 251 (2000).

[16] S. Furihata and T. Nakamura, Journal of Nuclear Science and Technology **Supplement 2**, 758 (2002).

[17] A. Kotov, L. Andronenko, M. Andronenko, Y. Gusev, K. Lukashin, W. Neubert, D. Seliverstov, I. Strakovsky, and L. Vaishnene, Nucl. Phys. A **583**, 575 (1995).

[18] S. V. J. Cugnon, C. Volant, Nucl. Phys. A **620**, 475 (1997).

[19] A. Boudard, J. Cugnon, S. Leray, and C. Volant, Phys. Rev. C **66**, 044615 (2002).

[20] G. Bertsch and S. D. Gupta, Phys. Reports **160**, 189 (1988).

[21] J. Aichelin, Phys. Reports **202**, 233 (1991).

[22] R. Charity, M. A. McMahan, G. J. Wozniak, R. J. McDonald, L. G. Moretto, D. G. Sarantites, L. G. Sobotka, G. Guarino, A. Pantaleo, L. Fiore, et al., Nucl. Phys. A **483**, 371 (1988).

[23] W.Cassing, private information.

[24] G. Westfall, J. Gosset, P. Johansen, A. Poskanzer, W. Meyer, H. Gutbrot, A. Sandoval, and R.Stock, Phys. Rev. Lett. **37**, 202 (1976).

[25] J. Aichelin, J. Hüfner, and R. Ibarra, Phys. Rev. C **30**, 107 (1984).

[26] G. Berlad, A. Dar, and G. Eilam, Phys. Rev. D **13**, 161 (1979).

[27] J. B. Cumming, Phys. Rev. Lett. **44**, 17 (1980).

[28] G. D. Westfall, R. G. Sextro, A. M. Poskanzer, A. M. Zebelman, G. W. Butler, and E. K. Hyde, Phys. Rev. C **17**, 1368 (1978).